A density matrix description of ^{14}N overtone nuclear magnetic resonance in static and spinning solids

Laura Marinelli, Sungsool Wi, and Lucio Frydman[a)]
Department of Chemistry, University of Illinois at Chicago, 845 West Taylor Street, Chicago, Illinois 60607

(Received 4 September 1998; accepted 6 November 1998)

Overtone NMR is an experiment introduced by LeGros, Bloom, Tycko, and Opella, capable of providing ^{14}N powder spectra devoid of first-order quadrupole broadenings by irradiation and observation of the nuclear spins at twice their Larmor frequency. This technique constitutes one of the most promising alternatives for the acquisition of high resolution solid ^{14}N NMR spectra from random powders, particularly if it can be combined with strategies capable of removing the substantial second-order quadrupole broadenings remaining in the overtone line shapes. In order to facilitate the search for these averaging manipulations, we present here a theoretical description of the overtone experiment based on the time-domain propagation of density matrices. It is shown that by combining perturbation methods with appropriate rotating-frame transformations and diagonalizations, overtone spin-1 phenomena can be described using a single set of fictitious spin-1/2 operators. By contrast to conventional spin-1/2 irradiation and detection processes, however, overtone manipulations involve an unusual angular dependence on the azimuthal angle defining rotations about the main Zeeman magnetic field. This behavior introduces unexpected complications toward the narrowing of overtone resonances by conventional sample spinning techniques. Nevertheless, it can still be shown that the removal of all spin-1 anisotropies by certain forms of dynamic-angle spinning overtone NMR remains feasible. © *1999 American Institute of Physics.* [S0021-9606(99)01806-1]

I. INTRODUCTION

Nuclear magnetic resonance (NMR) is one of the methods of choice for analyzing structural and dynamic problems over a wide range of polycrystalline or amorphous solids.[1,2] Much of this success arises from the development of a variety of time-dependent spin-manipulation techniques, which allow one to discriminate signals arising from inequivalent chemical sites in spite of the anisotropic character of high-field spin interactions. This coherent averaging of anisotropies was achieved decades ago for spin-1/2 systems via the introduction of magic-angle spinning (MAS) and of hetero- and homonuclear decoupling techniques.[3–6] Obtaining a similar degree of resolution proved more elusive for the important case of nuclei with spin $S \geqslant 1$ due to the sizable first- and second-order quadrupolar broadenings arising from interactions between these spins and their surrounding electric field gradients.[7] For the case of half-integer quadrupolar nuclei it had long been known that these anisotropies can be bypassed to first order by constraining the NMR observation to the central $-1/2 \leftrightarrow +1/2$ transition,[8] but only recently it has been shown that the second-order effects remaining in the spectra can be further removed by active averaging methods such as double rotation (DOR), dynamic-angle spinning (DAS), or multiple-quantum (MQ) MAS NMR.[9–13]

In spite of all these developments there is still an important isotope that so far has escaped from the realm of high resolution solids NMR; it is ^{14}N, a spin-1 nucleus. With a 99.6% natural abundance, this NMR-active nucleus is the most common of nitrogen's isotopes. Its two allowed Zeeman transitions, however, are subjected to large first- and second-order quadrupole effects, which have hitherto prevented ^{14}N NMR characterizations of inequivalent sites in powdered samples. Even in solution phase, ^{14}N spectroscopy is of limited use due to the strong line broadening caused by quadrupolar relaxation. Still, since in the case of solid samples individual single crystals are known to yield relatively sharp ^{14}N signals,[14] it should in principle be possible to retrieve high resolution spectra from their powders by using a suitable combination of coherent averaging techniques. A most promising starting point for the acquisition of such spectra is the pulsed overtone ^{14}N NMR experiment, an approach first demonstrated by LeGros and Bloom for the case of single crystals[15] and subsequently expanded and analyzed in detail by Tycko, Opella, and co-workers in connection with studies of powdered samples and of oriented systems.[16–20] At the center of this insightful experiment lies the idea of overcoming the nearly intractable excitation and detection challenges posed by the megahertz-wide first-order ^{14}N quadrupole broadenings by monitoring ''forbidden'' $+1 \leftrightarrow -1$ overtone transitions, whose magnetic dipole signals become directly observable by virtue of quadrupole-induced violations in the usual high-field $\Delta m = \pm 1$ NMR selection rule. This in turn leads to spectra that are solely affected by second-order quadrupole effects which although

a)Author to whom correspondence should be addressed. Electronic mail: lucio@samson.chem.uic.edu

large (10^4-10^5 Hz), could conceivably be scaled or even averaged away by manipulations of the spatial terms in the spin Hamiltonian.

At least two studies have discussed the feasibility of achieving distinctions among inequivalent sites with the aid of this type of line narrowing and overtone techniques. As part of their seminal work on ^{14}N overtone spectroscopy Tycko and Opella demonstrated that sample spinning has profound effects on the shape and resonance frequency of an overtone line shape, although the line narrowing that could have been expected on the basis of previous variable angle spinning NMR experiments did not materialize.[18] More recently, Takegoshi and Hikichi discussed the possibility of removing second-order broadenings by DAS and DOR methods, and concluded that whereas the former would not provide the expected line narrowing the latter could in principle have a chance to succeed.[21] Stimulated by these observations, we decided to revisit overtone NMR and focus on its possible combination with averaging techniques capable of sharpening the ^{14}N NMR lines. Previous studies have carried out similar analyses in the frequency domain, using a combination of perturbation theory for calculating the frequencies of the overtone transitions and transition moments for estimating the corresponding signal intensities.[18,21] By contrast we present here an analysis based on the time propagation of density matrices, which is the approach most frequently employed in interpretations of other types of time-dependent coherent averaging experiments.[22,23] For the case of static sample experiments (Sec. II) this procedure yields spectral predictions that are, when dealing with small excitation pulse widths and on-resonance irradiation, nearly coincident with those arising from the predictions of frequency-domain/transition-moment calculations. The time-domain treatment, however, also provides insight into the buildup of overtone coherences by rf irradiation under different conditions, describes the nutation distortions that can be expected under optimal signal-to-noise excitation, predicts the feasibility of storing and recalling overtone coherences even in powder samples with a relatively high degree of efficiency, and further clarifies a number of differences and similarities between time-domain overtone NMR and double-quantum NMR experiments. Upon considering the effects of sample rotation the density matrix analysis makes a number of distinct predictions (Sec. III), including one according to which spinning a sample will split an overtone powder pattern into several shifted centerbands and thus yield broader signals than static experiments for a majority of spinning angles. This phenomenon agrees well with the observations of Tycko and Opella, and it conspires against the successful use of MAS or DOR toward the line narrowing of overtone powder patterns. Nevertheless it is shown that these complications can be avoided by certain types of DAS experiments (Sec. IV), which by eliminating the spinning-induced splittings of the centerbands present a good opportunity for retrieving high resolution solid state ^{14}N NMR spectra from powdered samples.

II. THEORY OF OVERTONE NMR ON STATIC SAMPLES

This section introduces a time-domain density matrix description of the pulsed overtone NMR experiment as it applies to static ^{14}N spin ensembles, following in as much as possible the nomenclature and approximations employed in Refs. 15 and 18. Toward this end we will consider a $S=1$ spin ensemble consisting of isolated nuclei affected by Zeeman, quadrupolar, and chemical shift interactions, and which is occasionally acted upon by a rf field. The total laboratory frame spin Hamiltonian can in this case be expressed, in angular frequency units, as a sum of static internal and external interactions plus a time-dependent rf irradiation term.[7]

$$\mathcal{H}^{\rm lab}_{\rm total}=\mathcal{H}^{\rm lab}_{\rm static}+\mathcal{H}^{\rm lab}_{\rm rf}(t)=\mathcal{H}_Z+\mathcal{H}_Q+\mathcal{H}_{\rm cs}+\mathcal{H}^{\rm lab}_{\rm rf}(t), \quad (1)$$

where

$$\mathcal{H}_Z=-\gamma B_0 S_z=-\omega_0 S_z \quad (2)$$

denotes the usual Zeeman coupling to a static applied magnetic field B_0 assumed parallel to the z axis,

$$\mathcal{H}_Q=\omega_q[\sqrt{6}T^{\rm PAS}_{20}+\eta(T^{\rm PAS}_{22}+T^{\rm PAS}_{2-2})] \quad (3)$$

describes the untruncated quadrupolar interaction in its principal axes system in terms of the quadrupole frequency $\omega_q=(e^2qQ/h)/[4S(2S-1)]$ and of irreducible spherical tensor operators $\{T^{\rm PAS}_{2m}\}_{-2\leq m\leq 2}$, $\mathcal{H}_{\rm cs}$ is the full chemical shielding Hamiltonian, and

$$\mathcal{H}^{\rm lab}_{\rm rf}(t)=2\omega_1(S_x\sin\chi+S_z\cos\chi)\cos(\omega_{\rm irr}t+\phi) \quad (4)$$

describes the coupling between the spins and a monochromatic radiation possessing an oscillation frequency $\omega_{\rm irr}$, an amplitude $2\omega_1=2\gamma B_1$, a phase ϕ, and an arbitrary orientation χ with respect to the Zeeman field. Under the effects of this Hamiltonian the density matrix ρ describing the spin ensemble will evolve according to the Liouville–von Neumann equation

$$i\dot{\rho}=[\mathcal{H}^{\rm lab}_{\rm static}+\mathcal{H}^{\rm lab}_{\rm rf}(t),\rho] \quad (5)$$

starting from what will be assumed an initial state ρ_0.

The exact analytic integration of such an equation, involving 3×3 Hamiltonians that do not self-commute and are time dependent, is problematic. The usual approach to its resolution involves neglecting all elements that are nonsecular in the Zeeman representation, and then proceeding into a frame rotating at approximately $\omega_{\rm irr}$ in order to eliminate the time dependence included in $\mathcal{H}^{\rm lab}_{\rm rf}(t)$.[22] Both steps would be premature in the overtone treatment, which is known to rely on the nonsecular terms in the static Hamiltonian.[15–20] The integration of Eq. (5) can be simplified by following in the footsteps of previous overtone analyses and assuming that the quadrupolar interaction can be taken as a perturbation to the dominant Zeeman term.[15,18] This approximation is justified by the fact that typical ^{14}N quadrupole coupling frequencies are usually an order of magnitude smaller than their Zeeman counterparts (1–4 vs 10–40 MHz), and its validity has been extensively confirmed in related analyses of quadrupole-perturbed ^{13}C–^{14}N dipolar interactions.[24] With the aid of this assumption, standard perturbation theory can be exploited to calculate the tilting matrix $\mathcal{T}$ that diagonal-

izes the quadrupole-perturbed Hamiltonian $\mathcal{H}^{\text{lab}}_{\text{static}}$. Up to a second-order correction of the energy levels this matrix is given by[25]

$$\mathcal{T}=\begin{bmatrix} 1 & -\frac{\epsilon f^*}{\sqrt{2}} & \frac{\epsilon g}{2} \\ \frac{\epsilon f^*}{\sqrt{2}} & 1 & \frac{\epsilon f}{\sqrt{2}} \\ -\frac{\epsilon g^*}{2} & -\frac{\epsilon f}{\sqrt{2}} & 1 \end{bmatrix}, \tag{6}$$

where $\epsilon=\omega_q/\omega_0$ describes the ratio between the quadrupolar and Zeeman interactions, and *f*, *g* are complex geometric functions depending on the set of Euler angles (α, β, γ) relating the principal axes systems of the quadrupolar and the Zeeman interactions. These functions have been explicitly described by Tycko and Opella in their analysis of overtone spectroscopy,[18] and one of their most interesting features is a dependence on the usually irrelevant γ-angle defining rotations about the static Zeeman field:

$$f(\alpha,\beta,\gamma)=e^{i\gamma}F(\alpha,\beta), \tag{7a}$$

$$g(\alpha,\beta,\gamma)=e^{i2\gamma}G(\alpha,\beta), \tag{7b}$$

where as noted in Ref. 18

$$F(\alpha,\beta)=3\sin\beta\cos\beta-\eta(\cos 2\alpha\sin\beta\cos\beta + i\sin 2\alpha\sin\beta), \tag{8a}$$

$$G(\alpha,\beta)=(3/2)\sin^2\beta+\eta[\cos 2\alpha(1+\cos^2\beta)/2 + i\sin 2\alpha\cos\beta]. \tag{8b}$$

The $\mathcal{T}$ matrix carries in its columns the coefficients describing the quadrupole-perturbed eigenstates of a spin-1 system, which correspond to a ''corrected'' basis set in terms of which all spin operators involved in the overtone NMR experiment should be expressed. In other words, whereas in conventional high-field NMR it is sufficient to express the elements of any spin operator *O* in the usual Zeeman basis set

$$O_{mm'}=\langle m'|O|m\rangle, \tag{9}$$

the explicit consideration of first-order quadrupole effects requires implementing the additional transformation

$$O^T=\mathcal{T}^\dagger O\mathcal{T} \tag{10}$$

before carrying out any secular truncation of interactions. Application of this tilting transformation on $\mathcal{H}^{\text{lab}}_{\text{static}}$ results in a Hamiltonian $\mathcal{H}^T_{\text{static}}$,

$$\mathcal{H}^T_{\text{static}}=\begin{bmatrix} \omega^{(1)}+\omega^{(2)}+\omega_{\text{cs}}-\omega_0+O(\epsilon^3) & \epsilon(f^*-f)/\sqrt{2}+O(\epsilon^2,\epsilon^3) & -\epsilon g/2+O(\epsilon^3) \\ \epsilon(f-f^*)/\sqrt{2}+O(\epsilon^2,\epsilon^3) & -2\omega^{(1)}+O(\epsilon^3) & \epsilon(f-f^*)/\sqrt{2}+O(\epsilon^2,\epsilon^3) \\ -\epsilon g^*/2+O(\epsilon^3) & \epsilon(f^*-f)/\sqrt{2}+O(\epsilon^2,\epsilon^3) & \omega^{(1)}-\omega^{(2)}-\omega_{\text{cs}}+\omega_0+O(\epsilon^3) \end{bmatrix}, \tag{11}$$

where

$$\omega^{(1)}=\omega_q(3\cos^2\beta-1+\eta\cos 2\alpha\sin^2\beta)/2, \tag{12a}$$

$$\omega^{(2)}=\frac{\omega_q^2}{\omega_0}(|F|^2+|G|^2) \tag{12b}$$

are the so-called first- and second-order quadrupole effects, ω_{cs} includes the usual isotropic and anisotropic chemical shift terms, and $O(\epsilon^n)$ denotes terms of order *n* in a ω_q/ω_0 expansion.

In order to evaluate the effects that the radiation will have on a density matrix it is also necessary to express the rf term of the spin Hamiltonian in this tilted eigenstate base. This results in

$$\mathcal{H}^T_{\text{rf}}=\mathcal{T}^\dagger\mathcal{H}^{\text{Lab}}_{\text{rf}}\mathcal{T}=2\omega_1(S^T_x\sin\chi+S^T_z\cos\chi)\cos(\omega_{\text{irr}}t+\phi), \tag{13}$$

where the spin operators are now defined as

$$S^T_x=\mathcal{T}^\dagger S_x\mathcal{T} = \frac{1}{\sqrt{2}}\begin{bmatrix} \frac{\epsilon(f+f^*)}{\sqrt{2}} & 1-\frac{\epsilon g}{2} & \sqrt{2}\epsilon f \\ 1-\frac{\epsilon g^*}{2} & -\sqrt{2}\epsilon(f+f^*) & 1+\frac{\epsilon g}{2} \\ \sqrt{2}\epsilon f^* & 1+\frac{\epsilon g^*}{2} & \frac{\epsilon(f+f^*)}{\sqrt{2}} \end{bmatrix} \tag{14a}$$

and

$$S^T_z=\mathcal{T}^\dagger S_z\mathcal{T}=\begin{bmatrix} 1 & -\frac{\epsilon f^*}{\sqrt{2}} & \epsilon g \\ -\frac{\epsilon f}{\sqrt{2}} & 0 & \frac{\epsilon f^*}{\sqrt{2}} \\ \epsilon g^* & \frac{\epsilon f}{\sqrt{2}} & -1 \end{bmatrix}. \tag{14b}$$

These matrices show explicitly how the introduction of a quadrupole perturbation allows S_x and S_z to connect, through terms such as ϵf and ϵg, states that differ by two quantum numbers and which are normally devoid of direct magnetic dipole transitions.

To remove the time dependence still remaining in the tilted frame irradiation Hamiltonian [Eq. (13)] it is necessary to transform all the interactions into an appropriate rotating frame. This can be carried out by applying on all Hamiltonians a rotation of the spin operators about the z axis of the Zeeman interaction. This transformation will proceed, as usual,[22] at a rate ω_0, and is consequently defined by the operator

$$R=\exp(-i\omega_0 S_z)=\exp(i\omega_0\sqrt{2}T_{10}). \tag{15}$$

Transformation into the rotating frame yields the revised evolution equation

$$i\dot{\rho}_R=[\mathcal{H}^R_{\text{static}}+\mathcal{H}^R_{\text{rf}}-\omega_0\sqrt{2}T_{10},\rho_R], \tag{16}$$

where the rotating frame density matrix is

$$\rho_R=R^\dagger\rho^T R, \tag{17a}$$

the relevant part of the rotating frame static Hamiltonian will only involve its time-independent secular elements

$$\mathcal{H}^R_{\text{static}}=(R^\dagger\mathcal{H}^T_{\text{static}}R)_{\text{secular}}=\begin{bmatrix}\omega^{(1)}+\omega^{(2)}+\omega_{\text{cs}}-\omega_0 & 0 & 0\\ 0 & -2\omega^{(1)} & 0\\ 0 & 0 & \omega^{(1)}-\omega^{(2)}-\omega_{\text{cs}}+\omega_0\end{bmatrix}, \tag{17b}$$

and the rf interaction is

$$\mathcal{H}^R_{\text{rf}}(t)=R^\dagger\mathcal{H}^T_{\text{rf}}R=\omega_1(S^R_x\sin\chi+S^R_z\cos\chi)[\exp^{i(\omega_{\text{irr}}t+\phi)}+e^{-i(\omega_{\text{irr}}t+\phi)}]. \tag{17c}$$

The tilted/rotating frame operators $\{S^R_i\}_{i=x,z}$ in this rf Hamiltonian are time dependent because of the fast rotation that R imposes about T_{10}; the commutation relation

$$[T_{10},T_{km}]=mT_{km} \tag{18}$$

allows one to express these time dependencies as

$$S^R_x=R^\dagger S^T_x R=\frac{1}{\sqrt{2}}\begin{bmatrix}\dfrac{\epsilon(f+f^*)}{\sqrt{2}} & \left(1-\dfrac{\epsilon g}{2}\right)e^{-i\omega_0 t} & \sqrt{2}\epsilon f e^{-2i\omega_0 t}\\ \left(1-\dfrac{\epsilon g^*}{2}\right)e^{i\omega_0 t} & -\sqrt{2}\epsilon(f+f^*) & \left(1+\dfrac{\epsilon g}{2}\right)e^{-i\omega_0 t}\\ \sqrt{2}\epsilon f^* e^{2i\omega_0 t} & \left(1+\dfrac{\epsilon g^*}{2}\right)e^{i\omega_0 t} & \dfrac{\epsilon(f+f^*)}{\sqrt{2}}\end{bmatrix} \tag{19a}$$

and

$$S^R_z=R^\dagger S^T_z R=\begin{bmatrix}1 & -\dfrac{\epsilon f^*}{\sqrt{2}}e^{-i\omega_0 t} & \epsilon g e^{-2i\omega_0 t}\\ -\dfrac{\epsilon f}{\sqrt{2}}e^{i\omega_0 t} & 0 & \dfrac{\epsilon f^*}{\sqrt{2}}e^{-i\omega_0 t}\\ \epsilon g^* e^{2i\omega_0 t} & \dfrac{\epsilon f}{\sqrt{2}}e^{i\omega_0 t} & -1\end{bmatrix}. \tag{19b}$$

At this point it is justified to apply also on this rf Hamiltonian the usual secular approximation, according to which only the time independent matrix elements in the $\mathcal{H}^R_{\text{rf}}$ Hamiltonian need to be conserved. When irradiation occurs close to the overtone condition

$$\omega_{\text{irr}}\approx 2\omega_0, \tag{20}$$

this implies that the only terms that will be preserved in S^R_x, S^R_z are those situated two rows off the main diagonal [cf. Eq. (17c)]. In other words, the secular irradiation Hamiltonian will be given by

$$\mathcal{H}^R_{\text{rf}}=\omega_1\epsilon\begin{bmatrix}0 & 0 & (f\cos\chi+g\sin\chi)e^{i\phi}\\ 0 & 0 & 0\\ (f^*\cos\chi+g^*\sin\chi)e^{-i\phi} & 0 & 0\end{bmatrix}. \tag{21}$$

This treatment shows how, as indicated previously on the basis of transition moment analyses,[15,18] overtone irradiation is capable of connecting states differing by two quantum numbers through the absorption of radiation oscillating at twice the fundamental Larmor frequency. The fact that this density matrix derivation entailed a transformation into the usual rotating frame also stresses the fact that the coherent states excited by overtone irradiation are the same as those that will arise via conventional double-quantum time domain excitation,[26] even if this latter method does not require a tilting of the excitation

operators but involves rather the indirect connection of $|+1\rangle$ and $|-1\rangle$ states via single-quantum $|+1\rangle \leftrightarrow |0\rangle \leftrightarrow |-1\rangle$ transitions.[27] Because of this stepwise character double-quantum excitation cannot be properly described as a two-level process; the overtone rf Hamiltonian on the other hand connects exclusively the tilted $|+1\rangle$ and $|-1\rangle$ eigenstates and thus enables one to picture the corresponding density operator within this bidimensional subset of the original Liouville space. Furthermore, since first-order quadrupole effects affect these two states with equal strength regardless of a crystallite's orientation they can be ignored altogether, and the relevant overtone excitation Hamiltonian can be expressed in terms of a fictitious spin-1/2 Hamiltonian as

$$\mathcal{H}^R_{\text{excite}} = (\mathcal{H}^R_{\text{static}} + \mathcal{H}^R_{\text{rf}})_{|+1\rangle,|-1\rangle} = \begin{bmatrix} \omega_{\text{cs}} + \omega^{(2)} & \omega_1 \epsilon (f \cos\chi + g \sin\chi) e^{i\phi} \\ \omega_1 \epsilon (f^* \cos\chi + g^* \sin\chi) e^{-i\phi} & -\omega_{\text{cs}} - \omega^{(2)} \end{bmatrix}, \tag{22}$$

where the $\{|+1\rangle,|-1\rangle\}$ subscript stresses the contraction from an originally three-dimensional spin space to a now two-dimensional (2D) overtone space.

This Hamiltonian describes the overtone excitation in terms of a longitudinal ''off-resonance'' term arising from second-order quadrupolar plus chemical shift interactions, and of an ''irradiation'' field positioned in the $x-y$ plane of the rotating frame [Fig. 1(A)]. In spite of its simplicity there are peculiarities that differentiate this overtone excitation Hamiltonian from conventional spin-1/2 counterparts, some of which have already been noted on the basis of transition moment analyses.[15,18] One of them relates to the ϵ factor scaling the rf irradiation term; this reduces considerably the efficiency of the excitation field, will in general prevent the neglect of the off-resonance component, and may lead to substantial orientation-dependent nutation distortions. Also unusual is the behavior arising upon considering the evolution that $\mathcal{H}^R_{\text{excite}}$ imposes on the spin density matrix as a function of the excitation time τ. To appreciate this effect it will be assumed that at time zero the latter is given by

$$\rho_0 \cong \frac{\omega_0}{4kT} S_z = \alpha_B S_z, \tag{23}$$

that is, with spins aligned in a purely Zeeman thermal order. The spin evolution will then be determined by the eigenvalues λ_1, λ_2 of the nutation Hamiltonian

$$\lambda_1 = -\lambda_2 = \sqrt{(\omega_{\text{cs}} + \omega^{(2)})^2 + (\omega_1 \epsilon)^2 [|f|^2 \cos^2\chi + |g|^2 \sin^2\chi + \text{Re}(f^* g) \sin 2\chi]}, \tag{24}$$

and by its diagonalization matrix V,

$$V = \begin{bmatrix} \nu_1 & -\nu_2 \\ \nu_2^* & \nu_1 \end{bmatrix}, \tag{25}$$

where

$$\nu_1 = \frac{\omega_{\text{cs}} + \omega^{(2)} + \lambda_1}{\sqrt{2\lambda_1 (\omega_{\text{cs}} + \omega^{(2)} + \lambda_1)}}, \tag{26a}$$

and

$$\nu_2 = \frac{\omega_1 \epsilon (f \sin\chi + 2g \cos\chi) e^{i\phi}}{\sqrt{2\lambda_1 (\omega_{\text{cs}} + \omega^{(2)} + \lambda_1)}}. \tag{26b}$$

Integration of the time evolution equation [Eq. (16)] then results in the fictitious spin-1/2 density matrix

$$\rho_R(\tau) = \begin{bmatrix} \rho_{11} & \rho_{-11} \\ \rho_{1-1} & \rho_{-1-1} \end{bmatrix} \tag{27}$$

whose populations evolve as

$$\rho_{11} = -\rho_{-1-1} = \alpha_B [(|\nu_1|^2 - |\nu_2|^2)^2 + 4|\nu_1|^2 |\nu_2|^2 \cos(2\lambda_1 \tau)]/2 \tag{28a}$$

and its coherences as

$$\rho_{-11} = (\rho_{1-1})^* = \alpha_B \,\text{Re}(\nu_2^* \nu_1)[|\nu_1|^2 (1 - e^{2i\lambda_1 t}) - |\nu_2|^2 (1 - e^{2i\lambda_2 t})]. \tag{28b}$$

This equation shows a peculiar property of overtone excitation, as it predicts that the total spin coherence that will be excited by an overtone pulse over a powdered sample will be zero. Indeed the off-diagonal elements in $\rho_R(\tau)$ are proportional, through their linear ν_2 term, to the f and g functions

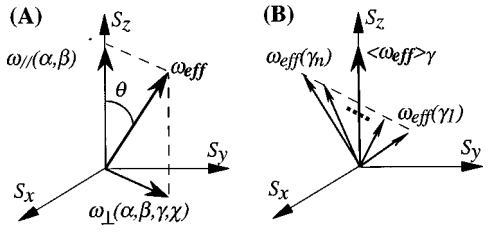

FIG. 1. Schematic representation of the nutation fields characterizing the excitation of coherences in overtone NMR. (A) Effective field corresponding to a single (α, β, γ) orientation between the quadrupolar and Zeeman tensors, characterized by a longitudinal component $\omega_{\|}$ and a transverse irradiation field $\omega_{\perp}$. When assuming ''typical'' ^{14}N site parameters and acquisition conditions ($e^2qQ/h = 3$ MHz, $\eta_q = 0$, $\omega_{\text{cs}} = 0$, $\omega_0/2\pi = 21$ MHz, rf field strength $\omega_1/2\pi = 150$ kHz, $\chi = 90°$), calculations predict an average powder nutation field $\omega_{\text{eff}}/2\pi \approx 68.5$ kHz and an inclination for this field $\theta \approx 9.1°$ for a single $\gamma = 0°$ value. (B) Overtone nutation fields characterizing a single (α, β) orientation and different γ angles between the Zeeman and quadrupolar tensors. The integrated excitation field $\langle\omega_{\text{eff}}\rangle_\gamma$ is in this case longitudinal, and the average coherence excited over the powder will consequently appear null.

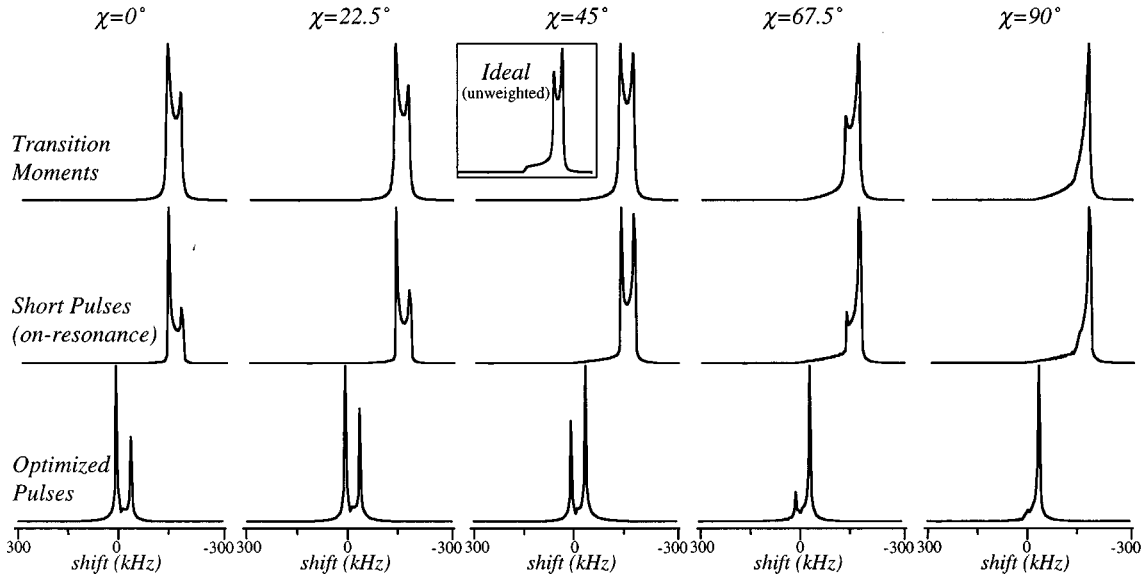

FIG. 2. Static ^{14}N overtone powder spectra predicted for a single ^{14}N site with coupling and acquisition parameters as described in Fig. 1, as a function of the indicated angles χ between the coil and B_0. Inset: Ideal $|+1\rangle\leftrightarrow|-1\rangle$ NMR spectrum expected solely on the basis of the orientation dependence of second-order effects; since the excitation and detection efficiencies of all crystallites are in this case assumed equal no χ dependence arises. Top row: NMR spectra calculated using a transition moment analysis according to which peak positions are given by the second-order quadrupolar frequency, and their intensities are weighted by the absolute square of the overtone transition moment $|\epsilon/2(f\cos\chi+g\sin\chi)|^2$. Center row: NMR spectra calculated after the full time domain propagation of the spin density matrix through the rf pulse and the free evolution, assuming a relatively short (5 μs) excitation pulse applied at the exact overtone condition $\omega_{irr}=2\omega_0$. Bottom row: NMR spectra calculated by the density matrix method for conditions that maximize the signal of the experiment ($\omega_{irr}=2\omega_0-70$ kHz, pulse width=30 μs—see Fig. 4); the absolute intensities of these spectra are an order of magnitude higher than those of the traces depicted in the center row. A thousand (β,γ) powder orientations were considered in these simulations.

which as noted above possess $e^{i\gamma}$ and $e^{2i\gamma}$ dependencies with respect to rotations about the Zeeman magnetic field [Eq. (7)]. The need to carry out for each (α,β) orientation of the quadrupolar tensor a sum over this γ angle, will therefore result in the apparent destructive cancellation of all $\{\rho_{1-1},\rho_{-11}\}$ off-diagonal elements when considering their excitation over a random powder [Fig. 1(B)].

In spite of this prediction, overtone signals have been collected not only from single crystals but also from polycrystalline samples. The feature that from a quantum mechanical point of view allows one to observe nonzero signals in the latter cases stems from the fact that the overtone free induction decay (FID) comes not as a result of calculating the expectation value $\langle S_+\rangle$ of the detection operator in the usual rotating frame, but from its value in the tilted/rotating frame introduced above. Indeed, the formalism leading to Eq. (28) can be extended to the evaluation of the magnetic dipole signals that spins will induce during their free evolution. When carried out in its entirety this calculation predicts the generation of an observable oscillating at twice the Larmor frequency and given by

$$S(t)=\mathrm{Tr}[e^{-i2(\omega_{cs}+\omega^{(2)})tS_z}\rho_R(\tau)e^{i2(\omega_{cs}+\omega^{(2)})tS_z}S_+^R], \quad (29)$$

where the exponential operators describe the evolution of $\rho_R(\tau)$ under the effects of the hitherto time-independent quadrupole and shielding interactions, and S_+^R is the overtone quadrature detection operator in the tilted rotating frame. It can be shown that the fictitious spin-1/2 matrix representing this operator is

$$S_+^R=\begin{bmatrix}0 & \frac{\epsilon}{2}(f\cos\chi+g\sin\chi)\\ 0 & 0\end{bmatrix}, \quad (30)$$

and when replaced into Eq. (29) this yields an analytic description of the single-pulse overtone FID which can be summarized as

$$S(t)=\epsilon^2c(\tau,\alpha,\beta,\gamma,\chi)e^{i2(\omega_{cs}+\omega^{(2)})t}[d_1(\alpha,\beta,\gamma)\sin^2\chi + d_2(\alpha,\beta,\gamma)\cos^2\chi+d_3(\alpha,\beta,\gamma)\sin 2\chi]. \quad (31)$$

This expression, further expanded in the Appendix, has been arranged so as to stress the FID's dependence on the irradiation angle χ. The c coefficient contains in it the excitation parameters, whereas the $\{d_i\}_{i=1-3}$ coefficients depend on the Euler angles orienting the Zeeman field with respect to the quadrupole tensor. The weighted integration of this signal over all powder orientations followed by a Fourier transformation leads to the nonzero spectral distributions shown in the center row of Fig. 2, calculated for a variety of excitation conditions as a function of the χ angle between the irradiation/detection coil and the external magnetic field B_0. Also shown in this Fig. 2 are the powder line shapes predicted by transition moment analyses like those originally presented by Tycko and Opella[18] and, for the sake of completeness, an ideal χ-independent second-order line shape such as the one characterizing a nutation-free excitation. As expected, line shapes derived from frequency domain transition moment analyses resemble the ones which will be observed upon using small excitation angles, but differ consid-

erably from the powder patterns that will result when employing pulsed NMR conditions that have been optimized for the highest signal-to-noise condition (Fig. 2, bottom row).

The overtone FID can also be rewritten as

$$S(t)=\epsilon^2 c(\tau,\alpha,\beta,\chi)e^{i2(\omega_{cs}+\omega^{(2)})t}\sum_{m=1}^{2}\sum_{n=1}^{2}[h_{mn}(\alpha,\beta,\chi)e^{im\gamma}\times\cos(n\gamma)+k_{mn}(\alpha,\beta,\chi)e^{im\gamma}\sin(n\gamma)], \quad (32)$$

where the coefficients involved are again listed in the Appendix. This expression allows one to appreciate why, in spite of the sinusoidal amplitude modulation imparted by the rf pulse exciting the overtone coherences, their signals are still observable even in the case of random powders: although overtone spin coherences acquire upon excitation $\{\cos(n\gamma),\sin(n\gamma)\}$ angular dependencies via the $\mathrm{Re}(\nu_2^*\nu_1)$ term in Eq. (28b), their demodulation by S_+^R endows them with additional $e^{i\gamma}$, $e^{i2\gamma}$ factors that will result in nonzero averages even after integration over the complete $0\leqslant\gamma\leqslant 2\pi$ sphere. By contrast, $|+1\rangle\leftrightarrow|-1\rangle$ coherences excited by conventional double-quantum Larmor irradiation lack the $\{\cos(n\gamma),\sin(n\gamma)\}$ angular dependence, and their signals will thus be unobservable by overtone NMR methods unless dealing with single crystals or with γ-oriented samples.[15] Conversely, $|+1\rangle\leftrightarrow|-1\rangle$ coherences excited from isotropic powders by overtone irradiation will not yield observable signals if one attempts to monitor them using the indirect detection scheme normally employed in 2D double-quantum NMR. To some extent it is possible to establish an analogy between these differing behaviors displayed by overtone and double-quantum coherences, and the more familiar situation arising when spin-1/2 coherences are excited by radially inhomogeneous B_1 gradients or by homogeneous B_1 rf fields (Fig. 3).[28] Also in these cases it is possible to obtain macroscopic NMR signals using either type of approach, provided that the same type of rf coil that is used for the excitation of the coherences is also used for the subsequent detection.[29] Furthermore, it has been shown that interesting effects can arise if during the excitation or the demodulation of the signal by means of a phase-inhomogeneous B_1 field spins undergo physical displacements, including irreversible decays in the case of random molecular displacements and time-dependent phase shifts if the molecular motions are coherent.[30] As is discussed in more detail in Sec. III, similar considerations apply to the case of overtone experiments provided that the dynamics involve molecular reorientations rather than a displacement of the spins.

Before concluding the static overtone analysis it is worth exploring the predictions that the density matrix treatment makes with regards to the relative efficiency with which overtone irradiation can excite $|+1\rangle\leftrightarrow|-1\rangle$ coherences under realistic conditions. A previous observation that is consistent with the time-domain calculations resulting from Eq. (31) relates to the improvement in signal intensity that can be expected with the introduction of off-resonance irradiation offsets [Fig. 4(A)].[18] Apparently, these offsets of the rf carrier frequency from the $2\omega_0$ overtone condition help compensate for the deleterious effects introduced by the dominant longitudinal second-order quadrupole term $\omega^{(2)}$ in the excitation of the coherences. An increase in the amount of excited overtone coherence is also brought about by using increasingly stronger rf field strengths [Fig. 4(B)]. According to these graphs it seems possible to excite, under favorable but realistic conditions, up to 25% of the maximum coher-

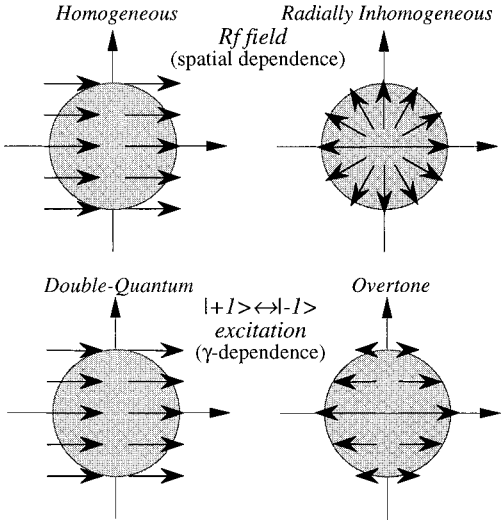

FIG. 3. Analogy between the B_1 field distributions generated by homogeneous or by radially inhomogeneous rf fields, and the transverse excitation fields characterizing conventional double-quantum or overtone spectroscopies. In the B_1 gradient case the rf excitation and the signal pickup profiles coincide, and are characterized by a simple radial dependence on the spatial positions. In the overtone case the excitation of coherences is characterized by $\{\cos(n\gamma),\sin(n\gamma)\}_{n=1,2}$ orientational dependencies and their detection by $\{e^{\pm in\gamma}\}_{n=1,2}$. In all cases, the presence of longitudinal offsets has been ignored.

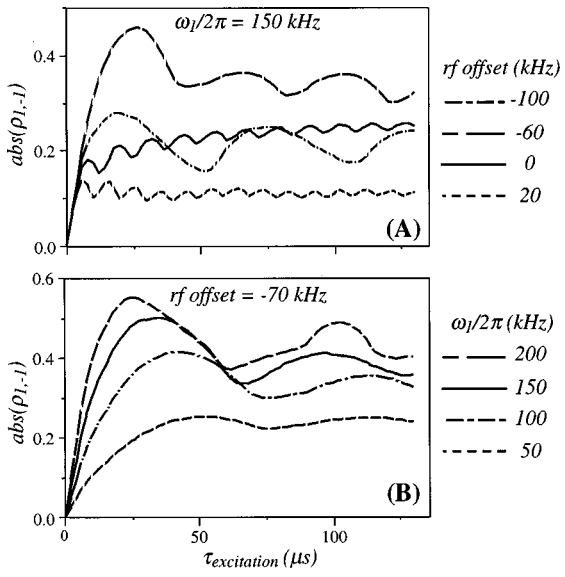

FIG. 4. Nutation behavior of the overtone coherence excitation as a function of (A) the rf irradiation offset with respect to $2\omega_0$; (B) the intensity of the rf irradiation field. Plots were obtained assuming an initial equilibrium density matrix $\rho_0=S_z$, the coupling and acquisition parameters listed in Fig. 1, and a $\chi=90°$ excitation/detection angle. A single $\gamma=0°$ value was considered in these calculations in order to avoid the destructive cancellation that would otherwise occur upon integration; other γ orientations were found to display qualitatively similar behaviors.

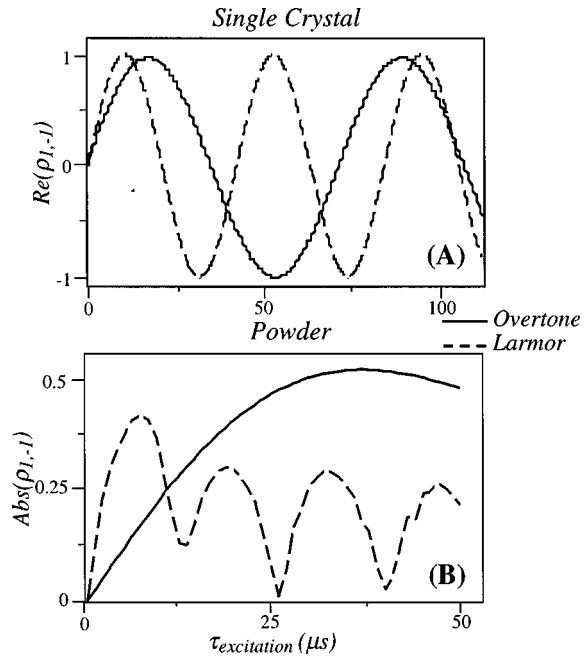

FIG. 5. Comparison between the nutation behaviors expected for the excitation of $|+1\rangle\leftrightarrow|-1\rangle$ coherences under the effects of an overtone pulse (—) and of a Larmor frequency pulse (---). All calculations assumed an initial $\rho_0=S_z$ equilibrium condition, as well as the coupling and acquisition parameters mentioned in Fig. 1. (A) Single crystal behavior calculated for $\beta=90°$, $\gamma=0°$; the overtone irradiation was considered at exactly $2\omega_0$. (B) Powdered sample behavior calculated for $\gamma=0°$ (to avoid destructive cancellation) and an overtone irradiation -70 kHz away from the exact $2\omega_0$ position [to maximize the powder signal, see Fig. 4(A)].

ence that can be expected from a quadrupole-free ^{14}N NMR experiment even when dealing with a powder. Unfortunately, the overtone signals that can be detected are still considerably attenuated due to both the ϵ factor appearing in the detection operator as well as due to partial cancellations occurring upon integrating over the γ angles; under optimized excitation conditions we found that the initial point of a powder overtone FID amounts to between 1% and 2% of the theoretical limit of its quadrupole-free Larmor counterpart. Nevertheless it is worth noting that because of the relative efficiency with which spins can be manipulated by overtone pulses and because of the two-level nature of this experiment it is feasible to follow the excitation of overtone coherences by their storage along the z axis, a manipulation that will be relevant when considering the possible application of DAS techniques to the narrowing of the overtone powder line shapes. Finally, since theory predicts that the $|+1\rangle\leftrightarrow|-1\rangle$ coherences that can be excited by either overtone irradiation or by double-quantum Larmor spectroscopy correspond to the same state (their density matrices are described in the same rotating frame), it is worth comparing the relative excitation efficiencies of these two experiments. For the case of a single crystal both methods can, under favorable conditions, achieve a complete transformation of the spin populations into transverse coherences [Fig. 5(A)], with the Larmor process being characterized by a faster nutation rate. When dealing with powdered samples the efficiency of on-resonance Larmor excitation is usually higher than that of on-resonance overtone excitation; an optimized off-resonance overtone irradiation, however, yields a larger amount of coherences than its optimized Larmor counterpart [Fig. 5(B)].

III. OVERTONE NMR ON ROTATING SOLIDS

The density matrix theory described in Sec. II provides a general framework for analyzing time-domain overtone NMR experiments on spin-1. Manipulations that would be particularly worth exploring are those which can scale down or even remove completely the anisotropic broadenings $\omega^{(2)}$ and ω_{cs} affecting the overtone spectra, as these would enable the implementation of high resolution ^{14}N NMR on random powders. A strategy that is widely used in NMR spectroscopy toward the achievement of this goal consists of rapidly spinning the sample at an angle with respect to the magnetic field B_0.[31,32] This approach was experimentally assayed by Tycko and Opella during the course of their comprehensive overtone NMR studies but it failed to reduce the linewidth of overtone powder patterns, and resulted instead in an apparent broadening and displacement of the signals.[18] We would like to discuss in this section how the density matrix formalism presented above predicts this unusual type of behavior.

In order to better point out the characteristics arising upon introducing sample spinning, the system to be considered here will be somewhat simplified compared to the one treated in Sec. II. We will assume that the spin-1 system excited by overtone irradiation is solely under the local action of a symmetric quadrupolar interaction, and that the excitation and signal demodulation are timed so as to have their relative rf phases equal to zero. The revised nutation Hamiltonian will therefore be given by

$$\mathcal{H}_{\text{total}}^{\text{lab}}=\mathcal{H}_Z+\mathcal{H}_Q+\mathcal{H}_{\text{rf}}^{\text{lab}} \tag{33a}$$

$$=-\omega_0 S_z+\omega_q\sqrt{6}T_{20}^{\text{PAS}}+2\omega_1(S_x\sin\chi+S_z\cos\chi)\times\cos(2\omega_0 t); \tag{33b}$$

furthermore it will be assumed that the spinning and the rf coil axes are collinear to each other and therefore χ will define both the rf axis of irradiation as well as the orientation of the spinner with respect to B_0.

As in the static case, the first step in this spinning overtone analysis consists of transforming the untruncated quadrupolar interaction from its principal axis frame into the principal system of the laboratory frame. This implies rewriting $\mathcal{H}_Q$ as[22]

$$\mathcal{H}_Q=\sum_{m=-2}^{2}(-1)^m T_{2m}R_{2-m}$$

$$=\omega_q[\sqrt{6}T_{20}a_S(t)+T_{21}f_S(t)-T_{2-1}f_S^*(t)+T_{22}g_S(t)+T_{2-2}g_S^*(t)], \tag{34}$$

where the leading term describes the usual first-order quadrupolar interaction, the f_S and g_S polynomials correspond to terms that will eventually define the tilting $\mathcal{T}$ matrix [Eq. (6)], and the S subscripts have been added to stress the fact these are now time-dependent functions corresponding to the spinning sample case. Now, however, we depart from the

static case, and instead of expressing these polynomials in term of a single set of Euler angles relating quadrupolar and Zeeman tensors these are written in terms of two subsequent rotations: a first one involving angles $\Omega_1=(\alpha,\beta,\gamma)$ and relating the quadrupolar system to a frame of reference fixed on the sample's rotor, and a second one transforming this spinning axis system into the laboratory frame via a time-dependent $\Omega_2=(\omega_r t,\chi,0)$ rotation. (As happens to be the case in conventional spin-1/2 sample spinning, the final azimuthal rotation in this Ω_2 transformation—corresponding to rotations of the axis of sample spinning about the B_0 field—is immaterial and can consequently be set to zero.) In terms of Wigner matrices $\{\mathcal{D}^{(2)}_{m,m'}\}_{-2\leqslant m,m'\leqslant 2}$ these transformations involve

$$a_S(t)=\sum_{n=-2}^{2}\mathcal{D}^{(2)}_{0,n}(\Omega_1)\mathcal{D}^{(2)}_{n,0}(\Omega_2), \tag{35a}$$

$$f_S(t)=\sum_{n=-2}^{2}\mathcal{D}^{(2)}_{0,n}(\Omega_1)\mathcal{D}^{(2)}_{n,-1}(\Omega_2),$$

$$f^*_S(t)=\sum_{n=-2}^{2}\mathcal{D}^{(2)}_{0,n}(\Omega_1)\mathcal{D}^{(2)}_{n,1}(\Omega_2), \tag{35b}$$

$$g_S(t)=\sum_{n=-2}^{2}\mathcal{D}^{(2)}_{0,n}(\Omega_1)\mathcal{D}^{(2)}_{n,-2}(\Omega_2),$$

$$g^*_S(t)=\sum_{n=-2}^{2}\mathcal{D}^{(2)}_{0,n}(\Omega_1)\mathcal{D}^{(2)}_{n,2}(\Omega_2). \tag{35c}$$

It is worth noting that in the absence of sample rotation the second of these tensor transformations can be set equal to unity and then the f_S, g_S functions will become equivalent to the *f*, *g* expressions appearing in the static case, except for the fact that in the latter case the (α,β,γ) angles describe the relation between quadrupolar and Zeeman axes systems.

It is now possible to exploit the fact that the frequency of sample rotation ω_r will in general be much smaller than any of the other relevant frequencies involved (ω_q, ω_0), in order to analyze the spinning overtone NMR experiment along the same lines that were set up above in the treatment of static samples. Indeed the slow rate of sample rotation justifies an adiabatic approximation whereby the spin system will behave at all moments as an eigenstate of the Laboratory frame Hamiltonian $\mathcal{H}_Z+\mathcal{H}_Q(t)$;[25] the spinning overtone analysis can then proceed as described for the static case albeit involving now a transformation into a slowly modulated tilted frame. This approach leads to the excitation of density matrix elements that are formally analogous to those given in Eqs. (24)–(28), but with the *f* and *g* functions replaced by $f_S(t)$ and $g_S(t)$. Similar arguments can be used in the derivation of the S^R_+ detection operator, which will now become

$$S^R_+(t)=\begin{bmatrix}0 & \frac{\epsilon}{2}[f_S(t)\cos\chi+g_S(t)\sin\chi]\\ 0 & 0\end{bmatrix}. \tag{36}$$

It can also be shown that even in this spinning case the γ dependence of the $f_S(t)$, $g_S(t)$ functions remains analogous to that characterizing the static sample experiment [Eq. (7)]:

$$f_S(t)=\sum_{n=-2}^{2}F_n(\beta,\chi)e^{in(\omega_r t+\gamma)}, \tag{37a}$$

$$g_S(t)=\sum_{n=-2}^{2}G_n(\beta,\chi)e^{in(\omega_r t+\gamma)}, \tag{37b}$$

where the complete expressions of $\{F_n,G_n\}_{-2\leqslant n\leqslant 2}$ are summarized in the Appendix.

The explicit time dependence that these equations predict for the S^R_+ operator is unusual, and will in turn result in hitherto unnoticed features in the overtone NMR spectra of spinning solids. Indeed, even if it is assumed that the spinning rate exceeds the strength of the overtone anisotropies (i.e., $\omega_r\gg\omega^{(2)}$), overtone signals will exhibit a time-oscillatory behavior arising from the modulation of their detection operator. This dependence will reflect in the FID as

$$S(t)=\epsilon^2 c(\tau,\alpha,\beta,\gamma,\chi)\exp\left[i2\int_\tau^t\omega^{(2)}(t')dt'\right]\times\sum_{m=-2}^{2}\sum_{n=0}^{2}H_{mn}(\beta,\chi)e^{im(\omega_r t+\gamma)}\cos(n\gamma), \tag{38}$$

where for the sake of simplicity we have disregarded the effects of sample spinning during the excitation of the powder overtone coherences (i.e., we have assumed an overtone pulse width τ much smaller than the rotor period $2\pi/\omega_r$). Equation (38), whose coefficients are detailed in the Appendix, is written in a format analogous to the one employed during the static analysis [Eq. (32)] in order to stress the fact that upon spinning, the $e^{im\gamma}$ factors associated with the signal detection will gain an additional $m\omega_r t$ time modulation. This in turn will split the original static powder pattern into a series of components positioned at 0, $\pm\omega_r$, and $\pm 2\omega_r$, which are unrelated to the usual spinning sidebands' manifolds arising from the time modulation of $\omega^{(2)}(t')$ or to Berry-type modulations of the spin quantization axis.[33] As can be appreciated from a comparison between the variable-angle-spinning spectra predicted by these time-domain signals and their static sample counterparts (Fig. 6), this extra phenomenon will result in most cases in an apparent broadening and an overall complication of the spectral line in spite of the ongoing scaling of second-order quadrupole anisotropies.

It may be instructive to briefly discuss the physical origin behind this behavior in terms of the simple radial B_1 gradient analogy introduced above. Toward this end consider an isolated spin-1/2 system confined in space and free from any internal interactions, whose magnetization has been excited by a 90° pulse into the *x* axis of its rotating frame [Fig. 7(A)]. Since spins in such a system are assumed confined to a small spatial region, their detection operator will not change appreciably over the sample volume and their signal will be detectable even by an inhomogeneous B_1 receiver coil; the resulting rotating-frame FID will thus look like a constant, and its signal will appear at zero frequency. If, however, the sample is now rotated at a rate ω_r about the symmetry axis of the B_1 field [Fig. 7(B)], the spin magnetization will appear to be executing a periodic motion with respect to the detection operator which for all practical pur-

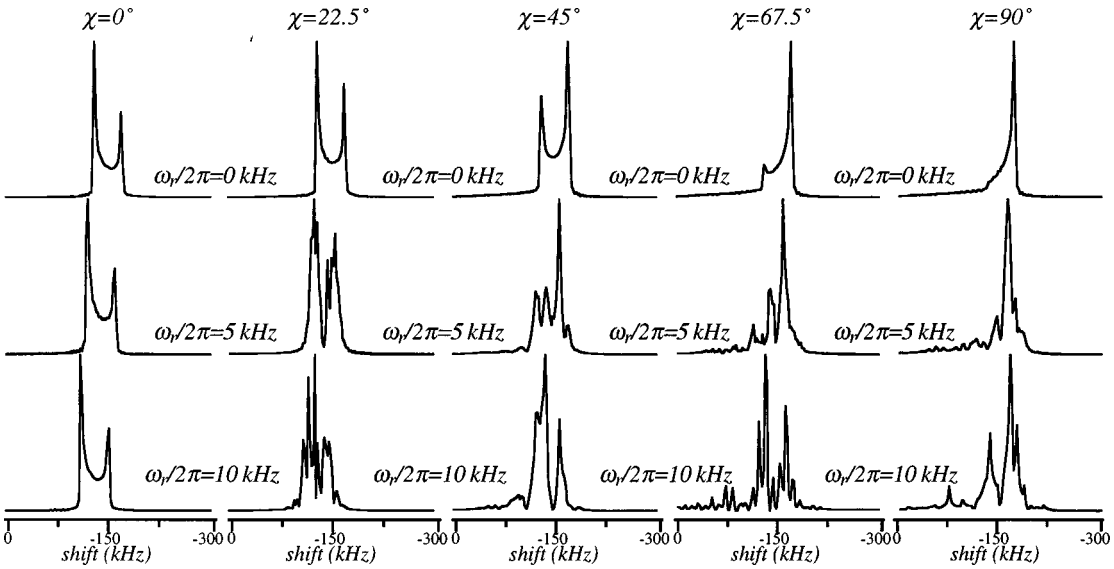

FIG. 6. Spinning speed dependence predicted for the overtone spectra as a function of different spinning/irradiation angles with respect to the external magnetic field. All calculations considered a single ^{14}N powder site with coupling and acquisition parameters as described in Fig. 1 and 1000 β and γ orientations. A 5 μs pulse placed at the exact overtone condition $\omega_{irr}=2\omega_0$ was considered in the excitation of the spins.

poses is indistinguishable from a rotating frame precession occurring at a frequency ω_r; after Fourier transformation, sample rotation will thus result in the resonance being shifted from its Larmor frequency by an offset ω_r. The same behavior will actually be observed if one considers not a small sample region but a sample occupying the complete volume of the coil, provided that the same spatially inhomogeneous B_1 coil that is used for the excitation is used for the signal detection and that the sample is rotated as a rigid body. This scenario is in fact very similar to the one occurring in overtone spectroscopy, except for the fact that inhomogenities are in this case generated by quadrupole interactions rather than by specially designed gradient coils, and thus their spinning rate dependencies are more complex than simply ω_r.

IV. REMOVAL OF SECOND-ORDER OVERTONE NMR ANISOTROPIES

As mentioned in Sec. I, one of the motivations for the present analysis was to explore the feasibility of retrieving isotropic solid state ^{14}N NMR spectra from powdered samples. To do so one could exploit overtone's built-in capability to bypass first-order quadrupole effects, but it is still necessary to combine this technique with some other method capable of removing the sizable second-order quadrupolar anisotropies remaining in its line shapes. Unfortunately, none of the schemes that have so far been successfully applied to the removal of these anisotropies in cases of half-integer quadrupolar nuclei appears to have a straightforward extrapolation to the case under consideration. Although MQMAS could be a potentially useful approach to the line narrowing of NMR spectra arising from integer spins with $S \geqslant 2$, its demand for two independent transitions that shall be simultaneously free from first-order quadrupolar broadenings prevents its utilization in $S=1$ cases like ^{14}N. The spinning characteristics described in Sec. III also deprive DOR from many potential applications, as they predict that overtone lines will split and shift by various multiples of both the inner and outer rotor spinning speeds during the course of the signal detection and thereby seriously complicate the resolution of chemically inequivalent sites. Similar complications should also affect overtone DAS experiments; yet as is discussed below, a more detailed analysis predicts that under certain conditions these complications will not be present and thus the acquisition of high resolution solid state ^{14}N NMR spectra should be feasible.

The sequence that we will consider toward the clarification of this issue is summarized in Fig. 8; it consists of an initial evolution period t_1 during which the sample is spun at an angle χ_1 with respect to the external field, a mixing time during which overtone coherences are stored while the rotating sample undergoes a mechanical realignment, and a final acquisition period t_2 during which the overtone signal is

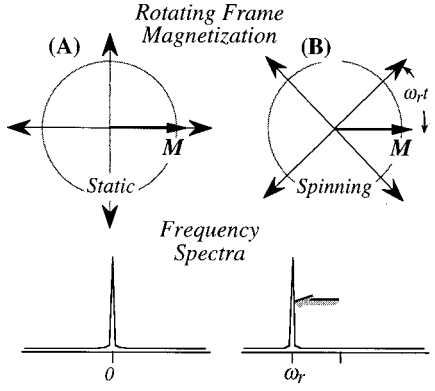

FIG. 7. Qualitative explanation for the peculiar shifts and splittings arising in overtone NMR upon sample spinning. In static cases (A) an on-resonance magnetization (the thick arrow), once excited, will not move with respect to the axes of its rotating frame (thin arrows) and thereby it will lead to a zero-frequency signal. Spinning the sample makes the axes of the rotating frame time dependent (B), and therefore even on-resonance magnetizations will appear to be precessing at a rate ω_r and result in offseted signals.

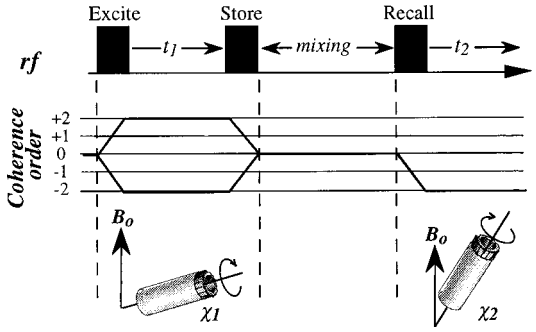

FIG. 8. The DAS NMR sequence considered in the study, analogous to the one normally employed for the sharpening of half-integer quadrupole resonances except for its use of overtone NMR pulses.

monitored while the sample is spun about an axis χ_2. Following the guidelines established for the analysis of half-integer quadrupolar nuclei,[10,34] the only angles $\{\chi_1,\chi_2\}$ that will be considered correspond to combinations capable of simultaneously removing all anisotropies arising from the first-order shielding and second-order quadrupolar interactions; dipolar couplings will be assumed negligible or being suppressed by decoupling means. A question that might arise upon considering such a sequence concerns the exact meaning of ''storing'' and ''recalling'' overtone coherences; as discussed in Sec. II, however, overtone experiments can be accurately pictured in terms of conventional $\{S_x,S_y,S_z\}$ spin-1/2 operators, for which the meaning of these processes is clear. Also worth noting is the fact that $\pm n\omega_r$ shifts associated with the time dependence of the overtone detection operator due to sample spinning (Sec. III) will not be active during the t_1 evolution period, since as is customary in 2D NMR these coherences will not be directly detected as voltages but rather encoded indirectly via their modulations of the final signal amplitude.[35] Strong spinning sidebands can still be expected along the indirect frequency domain owing to a t_1-dependent modulation of the excitation and storage rf Hamiltonians similar to the one that has recently been identified in MQMAS NMR;[36,37] this, however, will not constitute a severe line broadening mechanism and as it is shown by the simulations below its presence can well be tolerated.

The appearance for each chemical site of multiple powder patterns along the directly detected domain still constitutes an obstacle that needs to be overcome. To do so it is instructive to analyze the $S(t_1,t_2)$ signals resulting at the conclusion of a DAS procedure for different sets of complementary DAS angles, taking as starting point Eq. (31). According to this expression, deduced for static samples but extendible in a straightforward manner to spinning cases, overtone signals can be expressed as a superposition of three sets of line shapes possessing different χ scaling behaviors ($\sin^2\chi$, $\cos^2\chi$, $\sin^2\chi$). For two values of χ, 0° and 90°, these multiple line shapes will simplify into a single set. Furthermore it can be shown that for $\chi=0°$ only the H_{11} term in Eq. (38) is different from zero, and this leads to a resonance that is in shape identical to a nonspinning powder pattern but shifted from the latter by the spinning speed ω_r. No additional spinning sidebands are expected under these conditions due to the time independence of the $\omega^{(2)}$ interaction. Moreover, since $\{\chi_1=63°,\ \chi_2=0°\}$ constitutes a pair of complementary DAS angles, this solution appears as the optimum choice for achieving the complete removal of the overtone anisotropies. This speculation is validated by NMR calculations resulting from the full density matrix propagation of a spin system undergoing DAS (Fig. 9). In all cases, these calculations predict that long-lived time domain echoes will appear at the t_1/t_2 ratios predicted by the refocusing conditions of second-order anisotropies.[34,38] Even for a

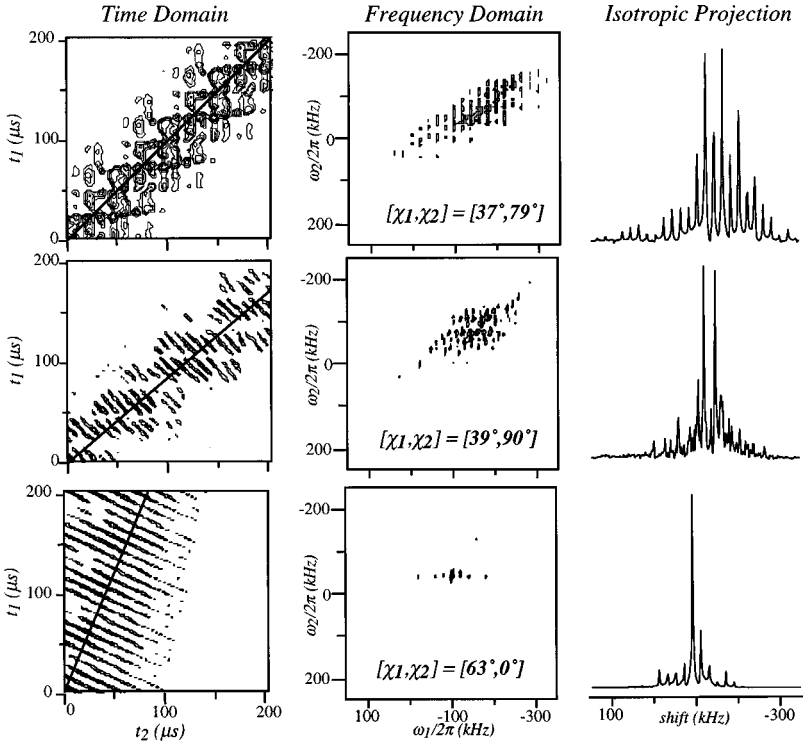

FIG. 9. DAS overtone NMR results calculated for the indicated pairs of complementary $\{\chi_1,\chi_2\}$ angles. The 2D time domain data sets (the left-hand column) were obtained by numerically propagating an initially equilibrated density matrix $\rho_0=S_z$ through all the stages of the experiment. A single ^{14}N powder site possessing the coupling and acquisition parameters described in Fig. 1 was considered, and sample spinning was assumed at 20 kHz. The thick lines inside each set describe the slopes expected for the second-order quadrupole echoes (1, 0.8, and 5, respectively). The 2D frequency domain spectra (the center column) illustrate the results expected after Fourier processing and shearing the time domain data; the result of projecting each of these data sets into their isotropic dimensions leads to the spectra (magnitude) shown in the right-hand column.

single ^{14}N powder site, however, a multitude of spinning sidebands can be observed for all 2D NMR spectra except for the one involving the $\{\chi_1=63°,\ \chi_2=0°\}$ combination. This implies that all other DAS alternatives will be unsuitable for the resolution of inequivalent sites in a sample, mainly by virtue of the spinning-induced shifts and splittings that characterize the overtone signal acquisition.

V. CONCLUSIONS

The present work described an extension of well-established theoretical methods involving the time propagation of density matrices to the evaluation of the ^{14}N overtone NMR experiment. As expected, the predictions made by this time-domain approach coincide with those of previously described transition moment analyses when dealing with single-pulse experiments performed on nonspinning samples and involving short excitation pulses. Density matrices, however, also provide the framework which is needed for the evaluation of more complex coherent manipulations of the spins; as examples of these applications we have discussed optimized single-pulse excitation conditions, differences, and similarities between time-domain multiple-quantum and overtone methods, the possibility of exciting as well as storing evolving overtone coherences, the effects of variable-angle sample spinning on overtone spectra, and the feasibility of improving the spectral resolution by overtone DAS NMR. We also expect this density matrix analysis to serve as a suitable starting point for the detailed evaluation of other types of coherent manipulations including sensitivity enhancement procedures based on cross polarization, the combined use of overtone and multiple-quantum strategies, and the implementation of overtone composite pulses.[15,16,39,40] Theoretical and experimental investigations of these procedures are currently under way.

ACKNOWLEDGMENTS

This work was supported by the National Science Foundation through Grant Nos. DMR-9420458 and CHE-9502644 (CAREER Award). L.M. acknowledges UIC for a University Fellowship. L.F. is a Beckman Young Investigator (1996–1998), Camille Dreyfus Teacher–Scholar (1996–2001), University of Illinois Junior Scholar (1997–2000), Alfred P. Sloan Fellow (1997–2000).

APPENDIX

We summarize here the expressions of the various polynomials and functions introduced in Eqs. (31), (32), (37), and (38).

The coefficients involved in the χ-dependent description of the static overtone FID [Eq. (31)] are

$$c(\tau,\alpha,\beta,\gamma,\chi)=\frac{\alpha_B\omega_1}{2\lambda_1}\{|\nu_1|^2[1-\exp(2i\lambda_1\tau)] - |\nu_2|^2[1-\exp(2i\lambda_2\tau)]\}, \quad \text{(A1)}$$

$$d_1(\alpha,\beta,\gamma)=\{[3\sin^2\beta+\eta\cos 2\alpha(1+\cos^2\beta)]\cos 2\gamma - 2\eta\sin 2\alpha\cos\beta\sin 2\gamma\}g(\alpha,\beta,\gamma), \quad \text{(A2)}$$

$$d_2(\alpha,\beta,\gamma)=[\tfrac{1}{2}\sin 2\beta(3-\eta\cos 2\alpha)\cos\gamma - \eta\sin 2\alpha\sin\beta\sin\gamma]f(\alpha,\beta,\gamma), \quad \text{(A3)}$$

$$d_3(\alpha,\beta,\gamma)=\tfrac{1}{2}\{[\tfrac{1}{2}\sin 2\beta(3-\eta\cos 2\alpha)\cos\gamma - \eta\sin 2\alpha\sin\beta\sin\gamma]g(\alpha,\beta,\gamma) + [(3\sin^2\beta+\eta\cos 2\alpha(1+\cos^2\beta)) \times\cos 2\gamma-2\eta\sin 2\alpha\cos\beta\sin 2\gamma] \times f(\alpha,\beta,\gamma)\}, \quad \text{(A4)}$$

where the definitions of f, g, α_B, λ_1, λ_2, ν_1, and ν_2 are given in Eqs. (7), (23), (24), and (26).

In addition to the c coefficient introduced in Eq. (A1), the coefficients required to rewrite the single pulse overtone FID in terms of its explicit γ dependencies [Eq. (32)] are

$$h_{11}(\alpha,\beta,\chi)=\tfrac{1}{2}\sin 2\beta(3-\eta\cos 2\alpha)\cos^2\chi F(\alpha,\beta), \quad \text{(A5)}$$

$$h_{12}(\alpha,\beta,\chi)=\tfrac{1}{2}[3\sin^2\beta+\eta\cos 2\alpha(1+\cos^2\beta)] \times\sin 2\chi F(\alpha,\beta), \quad \text{(A6)}$$

$$h_{21}(\alpha,\beta,\chi)=\tfrac{1}{4}\sin 2\beta(3-\eta\cos 2\alpha)\sin 2\chi G(\alpha,\beta), \quad \text{(A7)}$$

$$h_{22}(\alpha,\beta,\chi)=[3\sin^2\beta+\eta\cos 2\alpha(1+\cos^2\beta)] \times\sin^2\chi G(\alpha,\beta), \quad \text{(A8)}$$

$$k_{11}(\alpha,\beta,\chi)=-\eta\sin 2\alpha\sin\beta\cos^2\chi F(\alpha,\beta), \quad \text{(A9)}$$

$$k_{12}(\alpha,\beta,\chi)=-\eta\sin 2\alpha\cos\beta\sin 2\chi F(\alpha,\beta), \quad \text{(A10)}$$

$$k_{21}(\alpha,\beta,\chi)=-\tfrac{1}{2}\eta\sin 2\alpha\sin\beta\sin 2\chi G(\alpha,\beta), \quad \text{(A11)}$$

$$k_{22}(\alpha,\beta,\chi)=-2\eta\sin 2\alpha\cos\beta\sin^2\chi G(\alpha,\beta), \quad \text{(A12)}$$

where the definitions of F, G are given in Eq. (8).

The functions that are needed for describing the time dependencies of $f_S(t)$, $g_S(t)(\eta=0)$ in the case of a rotating sample [Eq. (37)] are

$$F_0(\beta,\chi)=\tfrac{3}{4}(3\cos^2\beta-1)\sin 2\chi, \quad \text{(A13)}$$

$$F_1(\beta,\chi)=\tfrac{3}{4}\sin 2\beta(\cos 2\chi+\cos\chi), \quad \text{(A14)}$$

$$F_{-1}(\beta,\chi)=\tfrac{3}{4}\sin 2\beta(\cos 2\chi-\cos\chi), \quad \text{(A15)}$$

$$F_2(\beta,\chi)=-\tfrac{3}{8}\sin^2\beta(\sin 2\chi+2\sin\chi), \quad \text{(A16)}$$

$$F_{-2}(\beta,\chi)=-\tfrac{3}{8}\sin^2\beta(\sin 2\chi-2\sin\chi), \quad \text{(A17)}$$

$$G_0(\beta,\chi)=\tfrac{3}{2}(3\cos^2\beta-1)\sin^2\chi, \quad \text{(A18)}$$

$$G_1(\beta,\chi)=\tfrac{3}{4}\sin 2\beta(\sin 2\chi+2\sin\chi), \quad \text{(A19)}$$

$$G_{-1}(\beta,\chi)=\tfrac{3}{4}\sin 2\beta(\sin 2\chi-2\sin\chi), \quad \text{(A20)}$$

$$G_2(\beta,\chi)=3\sin^2\beta\cos^4(\chi/2), \quad \text{(A21)}$$

$$G_{-2}(\beta,\chi)=3\sin^2\beta\sin^4(\chi/2). \quad \text{(A22)}$$

Finally, the coefficients that are involved in the time-dependent description of the overtone FID upon sample spinning [Eq. (38)] are: $c(\tau,\alpha,\beta,\gamma,\chi)$ as in Eq. (A1) (because of the short-pulse-width assumption); then

$$H_{00}(\beta,\chi)=\tfrac{9}{4}(3\cos^2\beta-1)^2\sin^2\chi, \quad \text{(A23)}$$

$$H_{10}(\beta,\chi)=\tfrac{9}{8}(3\cos^2\beta-1)\sin 2\beta\sin\chi(\cos\chi+1+\sin^2\chi), \quad \text{(A24)}$$

$$H_{-10}(\beta,\chi)=\tfrac{9}{8}(3\cos^2\beta-1)\sin 2\beta\sin\chi(\cos\chi-1-\sin^2\chi), \quad \text{(A25)}$$

$$H_{20}(\beta,\chi)=\tfrac{9}{8}(3\cos^2\beta-1)\sin^2\beta\sin^2\chi(1+\cos\chi), \quad \text{(A26)}$$

$$H_{-20}(\beta,\chi)=\tfrac{9}{8}(3\cos^2\beta-1)\sin^2\beta\sin^2\chi(1-\cos\chi), \quad \text{(A27)}$$

$$H_{01}(\beta,\chi)=\tfrac{9}{8}(3\cos^2\beta-1)^2\sin 2\beta\sin 2\chi, \quad \text{(A28)}$$

$$H_{11}(\beta,\chi)=\tfrac{9}{8}\sin^2 2\beta\cos\chi(\cos\chi+1+\sin^2\chi), \quad \text{(A29)}$$

$$H_{-11}(\beta,\chi)=\tfrac{9}{8}\sin^2 2\beta\cos\chi(\cos\chi-1-\sin^2\chi), \quad \text{(A30)}$$

$$H_{21}(\beta,\chi)=\tfrac{9}{16}\sin 2\beta\sin^2\beta\sin 2\chi(1+\cos\chi), \quad \text{(A31)}$$

$$H_{-21}(\beta,\chi)=\tfrac{9}{16}\sin 2\beta\sin^2\beta\sin 2\chi(1-\cos\chi), \quad \text{(A32)}$$

$$H_{02}(\beta,\chi)=\tfrac{9}{4}(3\cos^2\beta-1)\sin^2\beta\sin^2\chi, \quad \text{(A33)}$$

$$H_{12}(\beta,\chi)=\tfrac{9}{8}\sin^2\beta\sin 2\beta\sin\chi(\cos\chi+1+\sin^2\chi), \quad \text{(A34)}$$

$$H_{-12}(\beta,\chi)=\tfrac{9}{8}\sin^2\beta\sin 2\beta\sin\chi(\cos\chi-1-\sin^2\chi), \quad \text{(A35)}$$

$$H_{22}(\beta,\chi)=\tfrac{9}{8}\sin^4\beta\sin^2\chi(1+\cos\chi), \quad \text{(A36)}$$

$$H_{-22}(\beta,\chi)=\tfrac{9}{8}\sin^4\beta\sin^2\chi(1-\cos\chi). \quad \text{(A37)}$$

[1] C. A. Fyfe, *Solid State NMR for Chemists* (CFC, Ontario, 1983).
[2] K. Schmidt-Rohr and H. W. Spiess, *Multidimensional Solid-State NMR and Polymers* (Academic, London, 1994).
[3] E. R. Andrew, A. Bradbury, and R. G. Eades, Nature (London) **182**, 1659 (1958).
[4] I. J. Lowe, Phys. Rev. Lett. **2**, 285 (1959).
[5] J. S. Waugh, L. M. Huber, and U. Haeberlen, Phys. Rev. Lett. **20**, 180 (1968).
[6] J. Schaefer and E. O. Stejskal, J. Am. Chem. Soc. **98**, 1031 (1976).
[7] A. Abragam, *The Principles of Nuclear Magnetism* (Oxford University Press, Oxford, 1985).
[8] M. H. Cohen and F. Reif, Solid State Phys. **5**, 321 (1957).
[9] A. Samoson, E. Lippmaa, and A. Pines, Mol. Phys. **65**, 1013 (1988).
[10] A. Llor and J. Virlet, Chem. Phys. Lett. **152**, 248 (1988).
[11] E. W. Wooten, K. T. Muller, and A. Pines, Acc. Chem. Res. **25**, 209 (1992).
[12] L. Frydman and J. S. Harwood, J. Am. Chem. Soc. **117**, 5367 (1995).
[13] A. Medek, J. S. Harwood, and L. Frydman, J. Am. Chem. Soc. **117**, 12779 (1995).
[14] R. A. Haberkorn, R. E. Stark, H. van Willigen, and R. G. Griffin, J. Am. Chem. Soc. **103**, 2534 (1981).
[15] M. Bloom and M. A. LeGros, Can. J. Phys. **64**, 1522 (1986).
[16] R. Tycko and S. J. Opella, J. Am. Chem. Soc. **108**, 3531 (1986).
[17] R. Tycko, P. L. Stewart, and S. J. Opella, J. Am. Chem. Soc. **108**, 5419 (1986).
[18] R. Tycko and S. J. Opella, J. Chem. Phys. **86**, 1761 (1987).
[19] P. L. Stewart, R. Tycko, and S. J. Opella, J. Chem. Soc., Faraday Trans. 1 **84**, 3803 (1988).
[20] R. Tycko, in *Encyclopedia of NMR*, edited by D. M. Grant and R. K. Harris (Wiley, Chichester, 1996), p. 3425.
[21] K. Takegoshi and K. Hikichi, Chem. Phys. Lett. **194**, 359 (1992).
[22] U. Haeberlen, *Advances in Magnetic Resonance*, Suppl. 1 (Academic, New York, 1976).
[23] C. P. Slichter, *Principles of Nuclear Magnetic Resonance* (Springer, New York, 1990).
[24] A. C. Olivieri, L. Frydman, and L. Diaz, J. Magn. Reson. **75**, 50 (1987).
[25] L. D. Landau, *Quantum Mechanics* (Pergamon, Oxford, 1991).
[26] G. Drobny, A. Pines, S. Sinton, D. P. Weitekamp, and D. Wemmer, Faraday Discuss. Chem. Soc. **13**, 49 (1979).
[27] S. Vega and A. Pines, J. Chem. Phys. **66**, 5624 (1977).
[28] D. G. Cory, F. H. Laukien, and W. E. Maas, Chem. Phys. Lett. **212**, 487 (1993).
[29] D. Canet, Prog. Nucl. Magn. Reson. Spectrosc. **30**, 101 (1997).
[30] P. T. Callaghan, *Principles of Nuclear Magnetic Resonance Microscopy* (Oxford University Press, Oxford, 1991).
[31] E. Kundla, A. Samoson, and E. Lippmaa, Chem. Phys. Lett. **83**, 229 (1981).
[32] S. Ganapathy, S. Schramm, and E. Oldfield, J. Chem. Phys. **77**, 4360 (1982).
[33] J. W. Zwanziger, M. Koenig, and A. Pines, Annu. Rev. Phys. Chem. **41**, 601 (1990).
[34] K. T. Mueller, B. Q. Sun, G. C. Chingas, J. W. Zwanziger, T. Terao, and A. Pines, J. Magn. Reson. **86**, 470 (1990).
[35] R. R. Ernst, G. Bodenhausen, and A. Wokaun, *Principles of Nuclear Magnetic Resonance in One and Two Dimensions* (Clarendon, Oxford, 1987).
[36] L. Marinelli and L. Frydman, Chem. Phys. Lett. **275**, 188 (1997).
[37] U. Friedrich, I. Schnell, S. P. Brown, A. Lupescu, D. E. Demco, and H. W. Spiess, Mol. Phys. (in press).
[38] E. W. Wooten, K. T. Muller, and A. Pines, Acc. Chem. Res. **25**, 209 (1992).
[39] D.-K. Lee and A. Ramamoorthy, Chem. Phys. Lett. **280**, 501 (1997).
[40] D.-K. Lee and A. Ramamoorthy, Chem. Phys. Lett. **286**, 398 (1998).